

# Power Network SCADA Quantum Communications: A Comparison of BB84, B92, E91, and SARG04 Quantum Key Distribution Protocols

Hillol Biswas

Kyriakos Zoiros

Department of Electrical and Computer Engineering,  
Democritus University of Thrace,  
Xanthi, Greece

## Abstract:

The current state, emerging trends, and practical challenges of optical fiber-based power network SCADA quantum communication must be addressed to fully utilise the technological platform's potential in real-world power system SCADA communications involving massive volumes of real-time data, as well as in managing, encoding, and applications such as quantum cryptography. Quantum key distribution (QKD) is an essential part of the cybersecurity paradigm for quantum communication. Even though quantum computing with individual circuits yields probabilistic outcomes for the problem at hand, real-world datasets are complex and challenging to handle, even with telemetry. When using the cybersecurity triad of availability, confidentiality, and integrity (CIA) in reverse order (AIC), availability is given priority in electric power networks. This research assesses the use of the BB84, E91, B92, and SARG04 cryptographic protocols by applying them to large, multivariate power-system SCADA datasets and comparing the outcomes. By leveraging the variety of QKD protocols available with quantum electronics hardware, this simulation work provides a promising avenue for developing frameworks and deploying SCADA/PMU networks in actual power systems.

**Keywords:** QKD, Optical fibre, Quantum Communication, cybersecurity, quantum hardware

## Introduction

As the smart grid entails bidirectional power and data flows, cybersecurity is a key component of power system operation, depending on its size and complexity. The complexity is multifaceted, and, given the growing cybersecurity landscape in this critical infrastructure domain, emerging threats and vulnerabilities are paramount. As quantum computing and related technologies have attracted significant research interest across academia and industry, quantum communication in power system operation has also attracted growing interest worldwide. Many utilities are considering implementing it experimentally, while research on quantum communication through optical fibre has also been expanding.

The Danish Grid, for instance, has installed optical fiber ground wire and optical fiber cable-based quantum key transmission for the electricity power system in the substation at Funen from the Frøslev converter station [1]. Research and application-oriented efforts on the use of quantum encryption in power systems and the utility sector are ongoing. In early February 2019, the fiber network controlled by EPB in Chattanooga, Tennessee, saw the implementation and demonstration of a trusted node QKD, which consists of two different QKD techniques [2], [3].

LANL developed hardware and software to enhance security and reduce costs for quantum communication nodes that deliver QKD. Oak Ridge National Laboratory's (ORNL) "Quantum Physics Secured Communications for the Energy Sector" (Q-Sens) project. The cost and distance limitations of QKD are addressed by Q-Sens, which provides new quantum protocols for data authentication [4]. Although the study limitation recognizes the insufficiency of data, which is crucial for any real-world power network multidisciplinary domain, a simulated attack that is centered on the load frequency center (LFC) and using a Quantum Machine Learning (QML) technique has been mentioned [5]. With ever-increasing data availability and processing, smart grid 2.0 is expected to facilitate quantum-variants-based steps toward a projected carbon-neutral goal around 2050 [6].

In the QKD protocol, the IKE algorithm is used by the sorting phase. Similar to the SARG04 protocol, the proposed method is more resilient to PNS attacks [7]. In QKD, once the error rate is low enough and a sufficient number of photons have been detected, a shared private key known only to the sender and the recipient can be generated. It explains how this cutting-edge technology and its different modalities could benefit the essential infrastructure of dams or hydropower plants [8]. To secure Geneva's smart grid networks, QKD technology was examined and evaluated in an operational environment. It used both conventional channels in grid networks and a direct connection with a 3.4 km-long dark fiber specifically constructed for QKD [9].

From communication to electrical power systems operations for protecting the grid, it is imperative that any identified application areas in the quantum regime ideally require a broad overview of domain knowledge, as they are intersectional across domains. As cyber attackers' growing sophistication becomes apparent, it is likely surprising that future cybersecurity breaches will not, in turn, entail quantum attacks.

The complexity of current communication in power networks requires installing optical fiber ground wire, typically 24-core to 96-core, over long-distance transmission lines, either overhead or underground. The OPGW terminates in the substation, where it is laid through a cable trench within the substation yard and control room. In the control room, Ethernet connections are made through the substation automation system communication panel and connect to other panels, such as transformers, bus couplers, and others, depending on the substation size and complexity. The complexity further increases when adhering to the respective monitoring, control, protection, and communication industry standards, usually based on ITU's various series.

Supervisory Control and Data Acquisition is referred to as SCADA. As the name suggests, it focuses on the supervisory level rather than providing full control. Because of this, it is a

software-only package installed on top of hardware it interfaces with, usually via PLCs or other commercial hardware modules. The majority of industrial processes, including those in steel production, nuclear and conventional electricity generation and distribution, chemistry, and some experimental facilities like nuclear fusion, use SCADA systems [10].

At reduced maintenance costs, automated substations can provide the data needed to keep the customer's power supply constant. The integration of intelligent electrical devices (such as circuit breakers, transformers, and relays) with the ability to track their operation is known as substation automation. Circuit breakers, for instance, can detect appropriate maintenance diagnostics and assess their contact resistance. Microprocessor-based relays, circuit breakers, transformers, and motor-operated air switches make up automated substations. These components are all under the control of a remotely accessible graphical user interface unit [11].

The SCADA framework comprises both software and hardware. The software consists of "Human Machine Interface (HMI)," a central database (Historian), and other user software, while the hardware consists of "Remote Terminal Units (RTU)," "Master Terminal Unit (MTU)," actuators, and sensors [12]. These programs offer a means of communication between software and hardware. Actuators and sensors are connected to the physical environment, which is then connected to RTUs. To monitor and operate the SCADA system, RTUs collect sensor data and transmit telemetry to the MTU [13]. It has components and communication protocols that frame its architecture; however, Power System SCADA and its protocols are unique to power system operations in electricity utility networks. Since the introduction of the IEC 61850 series over the last two decades, utilities worldwide have adopted this interface for power system monitoring, control, and protection. It maps to the OSI (Open Systems Interconnection) Model, a set of guidelines that describes how various computer systems interact across a network. The International Organization for Standardization (ISO) created the OSI Model. Each of the seven layers that make up the OSI Model has distinct roles and duties. This tiered approach enables collaboration among many devices and technologies. The OSI Model provides a clear framework for handling network issues and data transfer. Many utility domains use the OSI Model as a guide to comprehend how network systems work [14].

The work is organized into the following sections: Power Networks, SCADA Communication, and Cybersecurity towards the Quantum era, followed by the Various QKD and Power Networks SCADA Qiskit Simulations section. The results section presents the findings, followed by the discussion, and the conclusion section concludes the report.

## Power Networks SCADA Communication and Cybersecurity towards the Quantum Era

This section comprises sub-sections of optical fiber-based communication, intrusion detection and prevention systems (IDPS), operational technology security, and optical quantum communication and hardware, as given below:

## Optical Fiber-Based Communication

Although other channels, including aquatic, are also potential options in the optical fibre-based endeavor, communication channels can be either free-space, like satellite, or optical fiber-based. Since the infrastructure is already in place and optical fiber communication is ubiquitous, such as in the Internet backbone, optical fiber links are the most attractive route for sending high-dimensional quantum states over a free-space link. Numerous fiber types, such as single-mode fibres (SMFs), multi-mode fibres (MMFs) (which include few-mode and higher-order mode fibers), and multicore fibers (MCFs), which are unique fibers with numerous cores within the same cladding, can be used to propagate high-dimensional quantum states. Depending on the application, several types of fiber provide the best solution. For example, in data centers, where space is limited and a significant number of connections are required, the fiber footprint is critical. Therefore, employing MCFs is a very attractive choice.

In power system communication through optical fibre ground wire, typically ITU G.652 [15] compliant single-mode optical fibres are used. Table 2: ITU-T G.652.D attributes stipulate the specific values of fibres and cables, viz., mode field diameter, cladding diameter, core eccentricity error, cladding non-circularity, cut-off wavelength, microbending loss, proof stress, chromatic dispersion parameters, attenuation, and PMD coefficients.

As power transmission networks are predominantly overhead and exposed to bare atmosphere, a separate ITU recommendation [16] is also provided. *Recommendation ITU-T L.151 refers to the installation of optical fibre ground wire cable. It deals with the factors that should be considered in determining the characteristics of this type of cable, the apparatus that should be used, the precautions that should be taken in handling the reels, and the method that should be used to string the cable and joint it.*

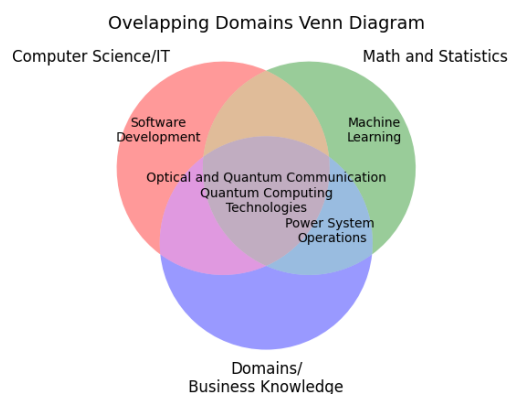


Fig. 1: Overlapping cum intersection domains of application

As the topic is an intersection of a few relevant domains [17] Fig. 1 illustrates the area of intersection of software/IT knowledge, artificial intelligence cum machine learning, and the power system operations, having sub-domains of optical and quantum communication, cyber security in operational technology (OT), quantum computing, and technologies of quantum hardware, i.e., quantum electronics sub-domain.

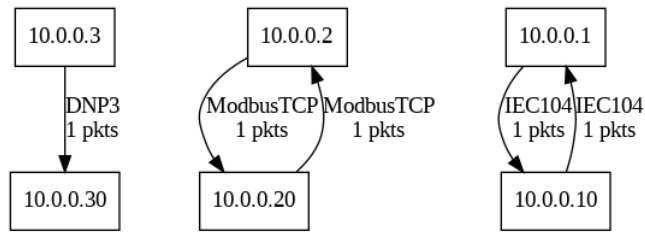


Fig. 2: SCADA three protocol sections

Fig. 2 depicts a typical master-to-RTU polling exchange with a single observed packet, shown by the unidirectional DNP3 communication flow from host 10.0.0.3 to 10.0.0.30 on the left side of the diagram. A typical client-server request-response transaction with one packet in each direction is depicted in the middle section, showing a bidirectional Modbus TCP connection between 10.0.0.2 and 10.0.0.20. A bidirectional IEC 60870-5-104 communication between 10.0.0.1 and 10.0.0.10 is shown on the right, representing a standard SCADA master-substation exchange in which a single packet is sent and received. When taken as a whole, the figure shows how several industrial control protocols can operate simultaneously within a single network segment. From cybersecurity paradigm, each protocol being active simultaneously have own weakness though.

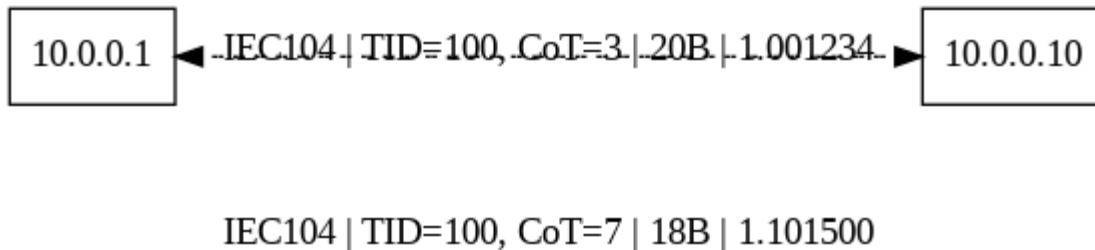


Fig. 3: IEC 104 sequence graph

An IEC 60870-5-104 communication exchange between 10.0.0.1 and 10.0.0.10 is depicted in the Fig. 3. A command or interrogation-related transmission is indicated by the message's Type Identifier (TID) = 100, Cause of Transmission (CoT) = 3, payload size of 20 bytes, and timestamp 1.001234. With TID = 100 and CoT = 7 (18 bytes, timestamp 1.101500), a matching IEC 104 frame indicates a follow-up response or activation confirmation. When combined, the exchange exemplifies a standard IEC 104 request-response exchange in a communication link between a SCADA master and substation.



*Fig. 4: A typical SCADA Substation Automation System Panel Inside*

A typical SCADA substation panel inside is dedicated to SCADA communication and control. The SCADA communication and control panel's internal layout is depicted in Fig. 4. It includes several industrial control modules, communication devices, protection relays, and terminal blocks installed on DIN rails. Relays, terminal strips, and circuit protection components are arranged in the right portion, while power/communication modules with Ethernet and field wiring connections are in the left. A standard industrial control cabinet design that facilitates remote monitoring, control signalling, and protocol-based communication (e.g., IEC 104, Modbus, DNP3) between field devices and the control centre is shown by the structured cable routing and segregation.

Together, the cabinet image depicts the actual electrical equipment that creates and handles these connections, whereas the previous network diagrams show the logical SCADA protocol exchanges (IEC 104, Modbus TCP, DNP3). RTUs, PLCs, communication processors, and power conditioning units are among the hardware modules that make up the panel's electronics layer, which connects field signals to IP-based industrial protocols. As a result, the network diagrams' protocol-level traffic clearly represents the electronic control and communication hardware located inside the SCADA panel.

## Intrusion Detection and Prevention Systems (IDPS)

Monitoring events in a computer system or network and examining them for indications of potential incidents—violations or impending threats of violations — of computer security regulations, acceptable use standards, or standard security practices is known as intrusion detection. Software that automates the intrusion detection process is known as an intrusion detection system (IDS). Software that combines the features of an intrusion detection system with the ability to prevent such occurrences is known as an intrusion prevention system (IPS). Many features of IDS and IPS technologies are similar, and administrators often disable preventive measures in IPS systems to make them behave more like IDSs. Thus, intrusion detection and prevention systems (IDPS) is a phrase that is commonly used for brevity [18]. These typically Globally, TCP/IP is a popular protocol for network communications. The OSI

model's application, transport, network, and data link layers are the four levels that make up TCP/IP communications.

To spot suspicious activity, a network-based IDPS examines network, transport, and application protocols while monitoring network traffic for specific network segments or devices. To find incidents, IDPS technologies employ a variety of techniques. The three main categories of detection techniques are stateful protocol analysis, anomaly-based detection, and signature-based detection. To enable more thorough and precise detection, the majority of IDPS solutions employ a variety of detection techniques, either independently or in combination [18].

### Operational Technology (OT) Security

SCADA operation via manipulated code can cause potential harm to power system operations and associated equipment, as demonstrated by the Aurora simulation in 2007 [19]. Unlike information technology (IT), power networks must be protected for operational technology. Thus, the conventional confidentiality, integrity, and availability (CIA) triad in IT cybersecurity ecosystems is usually applied in reverse order, with electric power availability prioritized on a 24/7 basis. However, over time, it appeared that SCADA power system operation cybersecurity is a complex intersection area of overlapping domains [17]. The cybersecurity scenario is rapidly evolving [20] as many cybersecurity incidents affecting power system infrastructure have been reported worldwide, involving one or more types. Although SCADA connectivity offers several advantages, like scalability, dependability, and remote connectivity, it also exposes a system that would otherwise be protected and isolated to unintended cybersecurity risks [21].

SCADA security analysis with sniffing tools, viz., Wireshark [21], Suricata [22], and Snort [23], has been researched for different messages for packet dissection [22] purposes. Although Suricata/Snort are generally used as intrusion detection and prevention systems, they do have packet sniffing/logging capabilities. In a real-world electricity utility, either of these, or a similar one, is often used for real-time situational awareness in a cybersecurity regime for telemetry packet analysis.

### Optical Quantum Communication and Hardware

While envisaging quantum communication through optical fibre, the following queries surfaced as follows:

#### 1) Why Optical Fibers Are Used in Quantum Communication

Since telecom optical fibers are compatible with current telecom infrastructure and offer low-loss transmission at about 1550 nm, they are perfect for quantum communication. They enable weak or coherent states, or single photons, to be sent to encode quantum information in QKD systems [23], [24].

#### 2) Essential Elements of a Fiber QKD Connection

A low-loss single-mode telecom fibre channel (~0.2 dB/km at 1550 nm), a quantum source (single photons, weak coherent pulses, or squeezed/coherent states), encoding techniques (polarization, phase, time-bin, or quadrature), and detectors (InGaAs APDs or SNSPDs) make up a fibre QKD system. The final

secret key is obtained via traditional post-processing, including filtering, parameter estimation, reconciliation, and privacy amplification [23].

### 3) Procedures

The most developed fiber-based method, DV-QKD (e.g., BB84 and decoy-state BB84), employs weak pulses or single photons [25].

Under ideal conditions, CV-QKD has exhibited distances of hundreds of kilometers and integrates well with telecom components. It uses homodyne/heterodyne detection and encodes information in optical quadratures [26], [27].

Advanced network- and device-independent ideas are supported by entanglement-based protocols (BBM92) [23].

Recent studies have extended the practical range, and MDI-QKD and twin-field protocols improve long-distance scaling and security against detector attacks [28].

### 4) Important Rate and Distance Restrictions

Exponential attenuation, detector dark counts, channel noise (particularly important in CV-QKD), and reconciliation inefficiencies are the main factors limiting fiber QKD performance. Secure key rates are further decreased by finite-size effects. Ultralow-loss fibres, high-performance detectors (such SNSPDs), or reliable intermediate nodes are frequently used for long-distance demonstrations [4], [3].

### 5) Distance Restrictions and Deployment Milestones

Photonic integration is progressively supporting operational QKD lines over intercity and metropolitan distances (tens to hundreds of km) [1].

Several hundred kilometres have been demonstrated in the field, including over 410 km of fibre transmission in the UK testbed for safe real-world applications [4], [29].

Trusted nodes that segment links and re-encrypt keys are frequently used in realistic long-distance deployments.

### 6) Overview and Prospects of Quantum Repeaters [30]

By employing entanglement swapping and quantum memories, quantum repeaters aim to extend the range without measuring quantum states. Even though there have been many theoretical and experimental advancements, scalable, deployable repeaters are still under development and are not yet commercially feasible [31], [32].

### 7) Real-World Difficulties and Their Mitigation

Robust security proofs, MDI-QKD, decoy-state approaches, and better hardware design all help to reduce security concerns [3]. Filtering, wavelength planning, and power control are necessary to minimise Raman noise while coexisting with classical traffic [33]. For wider deployment, semiconductor devices and photonic

integrated circuits (PICs) seek to lower system size, cost, and power consumption [1].

#### 8) Standard Performance Indicators and Prospect

At 1550 nm, fiber loss is usually 0.17–0.25 dB/km (~20 dB over 100 km). Depending on the protocol and technology, secure key rates can vary from kbps in metro networks to less than 1 bps at very long distances [3], [34].

All things considered, the most developed quantum communication technique for implementation at short to intercity scales is optical-fiber QKD. While CV-QKD provides integration benefits, DV-QKD is more deployment-ready. While enhanced protocols (MDI, twin-field) and trusted-node topologies increase the practical reach, quantum repeaters are the long-term solution to the fundamentally limited distance imposed by exponential loss.

## Various QKD and Power Networks SCADA Data Qiskit Simulations

According to the Heisenberg Uncertainty Principle (1927) [35], any eavesdropper can be detected because measurement affects quantum states. Because arbitrary quantum states cannot be precisely replicated, the No-Cloning Theorem [36] (1982, Wootters & Zurek) forbids interception without discovery. Cryptographers were inspired by these ideas to investigate quantum key distribution (QKD) as an alternative to traditional key exchange.

Bassard asked whether quantum communication could be more effective than classical communication. According to Holevo's theorem, it is impossible to transmit more than  $n$  bits of classical information using  $n$  quantum bits, unless the two parties are entangled; otherwise, the number of classical bits that can be transmitted is at most twice  $n$ . In apparent contradiction, conventional methods cannot effectively reproduce quantum communication for specific distributed computational tasks [37].

Two or more parties attempt to minimize the number of classical bits transferred while computing a joint function of their private inputs in the classical communication model. The size of inputs and the laws of classical information flow set limits on efficiency. The parties may share entanglement or trade qubits in quantum communication. Although a qubit cannot carry more than one classical bit of information due to Holevo's theorem, quantum techniques can lessen the requirement for communication because [37]:

- i) More effective correlation encoding is made possible by quantum superposition.

- ii) Non-classical correlations made possible by entanglement eliminate the requirement for communication (for example, certain problems can be solved with fewer qubits than classical bits).

- iii) Quantum communication outperforms the best classical protocols in some tasks by an exponential margin.

Subsequently, several quantum protocols have emerged as given below:

Ghosh et al.'s SIGNCRYPTION technique for SCADA [38] uses the Quantum Information Toolkit in Python, noting that RSA's security is based on the difficulty of factoring large prime numbers. This scheme is generic and does not explicitly address power system operations or their inherent complexity. However, unlike classical approaches, a quantum algorithm can easily solve the factorization problem by using the superposition principle. A classical version of Grover's algorithm requires  $O(N)$ , whereas a quantum variant requires  $O(\sqrt{N})$  for an exhaustive search. Symmetric algorithms such as AES are weakened by Grover's quantum search method for prime number factorization [39], [40]. Any attempt to clone a quantum system introduces defects into the replicas' states. This is the outcome of a fundamental law of quantum physics, the no-cloning theorem, which underpins the security of quantum communications.

Any attempt to clone a quantum system introduces defects into the replicas' states. This is the outcome of a fundamental law of quantum physics, the no-cloning theorem, which underpins the security of quantum communications. Despite the ban on perfect duplicates, several ideal cloning procedures can reproduce a quantum state with maximal accuracy. At the boundary of the physical limit imposed by the no-cloning theorem and the Heisenberg uncertainty principle, optimum quantum cloning has been experimentally accomplished for low-dimensional photonic states. However, increasing the dimensionality of quantum systems is highly advantageous for quantum computation and communication protocols [41].

A framework that leverages QKD-based secure communication and QPUF-based intelligent device attestation is proposed for quantum-capable smart grid entities. Quantum systems and simulators from IBM and Rigetti Computing were used to assess the QPUF-QKD integrated framework [42].

Additionally, it suggests the Self-Defensive Post-Quantum Blockchain Architecture (SD-PQBA), which is intended to defend SCADA systems in smart cities from both traditional and cutting-edge cyberthreats [43].

There is an urgent need to strengthen security in Industrial Control Systems (ICS) Supervisory Control and Data Acquisition (SCADA) networks to protect industrial operations against cyberattacks. The work's objective is to suggest and assess low-tech security solutions to protect vital infrastructure assets [44].

Theoretical examination of threats and defenses was necessary for the cybersecurity of smart energy systems. A multi-factor study of information security features was significant for essential parts of contemporary energy systems, including SCADA, IoT, and CPSs [45].

SCADA comprises several architectures and protocols, including IEC 60870-101/104, Fieldbus, Profibus, and Distributed Network Protocol (DNP-3). In power system domains, the cybersecurity ecosystem is vast and intricate [46], [13], [47]. A new attack surface and vector in the future is not entirely implausible because the traditional SCADA cybersecurity strategy identified numerous problems, such as dataset availability, scope studies on intrusion detection and prevention, and incident response and reporting [48]. QKD via a fiber-optic communication channel is a blockchain-based smart grid communication method in SCADA systems [47].

The most common methods for cybersecurity applications in packet analysis within the IT regime are network traffic detection using sniffing tools such as Wireshark and TCPDump.

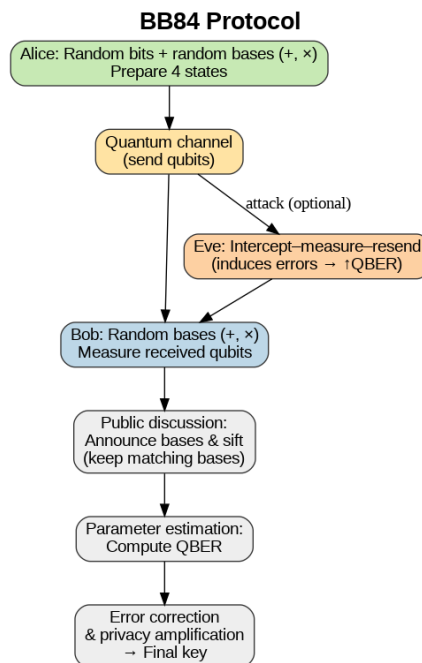
These tools can also be used for cybersecurity purposes, often in conjunction with other tools and artificial intelligence/machine learning applications, for intrusion detection within a real-time situational awareness context. The display of network security log data is a crucial topic for further study and advancement in network security monitoring [49]. To secure MMS communications in transport layer security, experiments were conducted using the Rivest-Shamir-Adleman (RSA) and Elliptic Curve Digital Signature Algorithm (ECDSA) algorithms for the signing of certificates with varying key sizes [50].

Table 1: Comparison Table of Quantum Communication Protocols

Protocol	Year	Key Idea	Basis States	Security Basis
BB84[51]	1984	Two conjugate bases	4	Heisenberg Uncertainty
B92[52]	1992	Two non-orthogonal states	2	State Indistinguishability
E91[53]	1991	Entanglement + Bell test	Entangled	Bell Inequality Violation
SGS04[54]	2004	Two-way qubit reuse	2	Ping-pong mechanism

This section further elucidates the approach for simulating BB84, B92, E91, and SGS04 protocols as given below:

## BB84



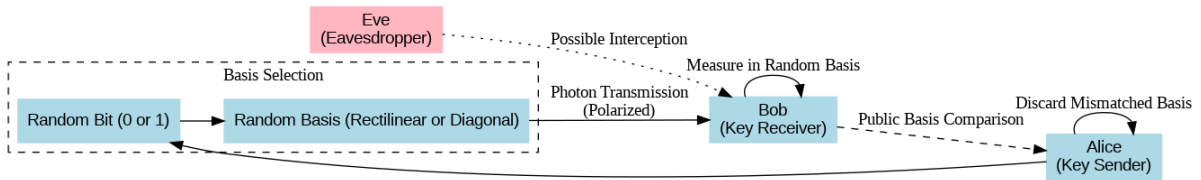


Fig. 5: BB84 Protocol

Fig. 5, the Four-State BB84 Protocol, which prepares and measures as Alice uses two mutually unbiased bases (+ and ×) to encode random bits into qubits. Bob uses randomly selected bases to measure each qubit. The final secure key is generated by applying error correction and privacy amplification, estimating QBER to detect eavesdropping, and keeping only matching-based results (sifting) after public basis comparison. Measurement disturbance and the no-cloning theorem are essential to security.

## B92

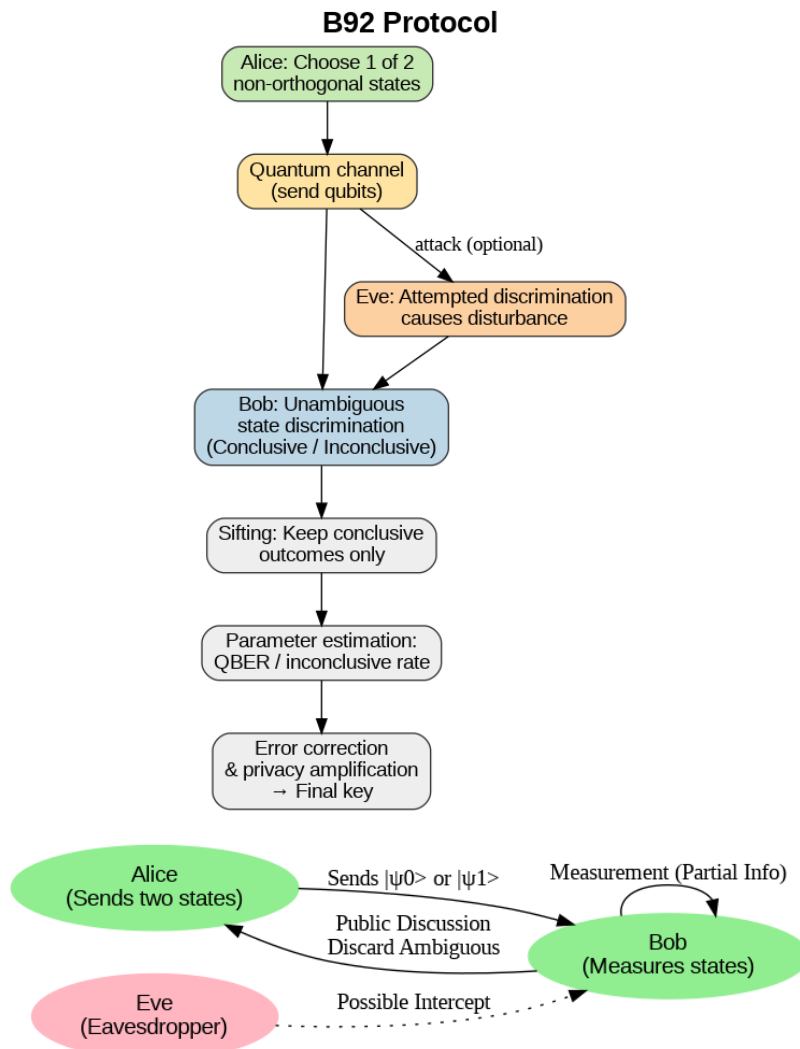


Fig. 6: B92 Protocol

Fig. 6, the Two Non-Orthogonal States under the B92 Protocol, uses just two non-orthogonal quantum states and streamlines BB84. Bob does clear state discrimination, yielding results that are either decisive or inconclusive. For key generation, only definitive results are retained. The final key is extracted using

traditional post-processing after any eavesdropping effort creates observable disruptions in the error or inconclusive rate.

## E91

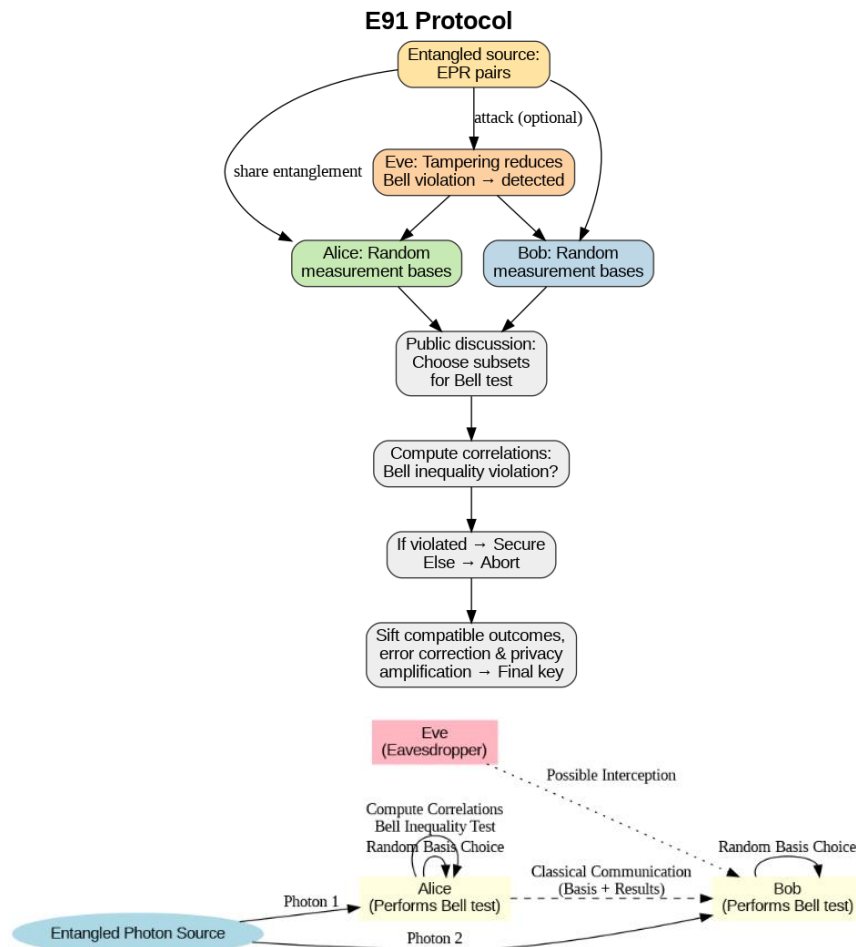


Fig. 7: E91 Protocol

Fig. 7, Entanglement-Based E91 Protocol (Bell-Test Security), depicts the method, as Alice and Bob divide up the entangled EPR pairs used by E91. A portion of the data is utilized to test for violations of Bell inequality, and both measures are taken on randomly selected bases. The channel is deemed secure if correlations defy Bell's inequality. The final key is produced by sorting and processing the remaining correlated results. Nonlocal correlations and quantum entanglement are the foundation of security.

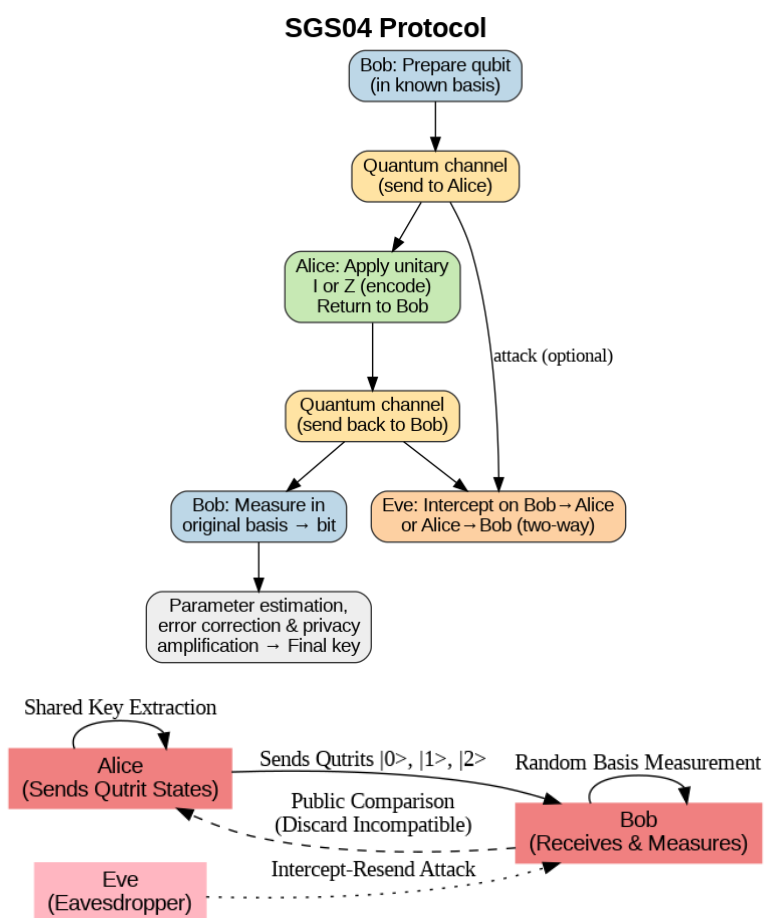


Fig. 8: SGS04 Protocol

Fig. 8, the Two-Way Deterministic QKD Protocol (SGS04), illustrates the approach as Bob produces a qubit and transmits it to Alice via the two-way SGS04 protocol. Alice does a unitary operation (I or Z) to encode data before returning it. Bob extracts the bit deterministically by measuring in the original basis. Before the final key is extracted, parameter estimation is essential to identify attacks on either path, since the qubit travels twice.

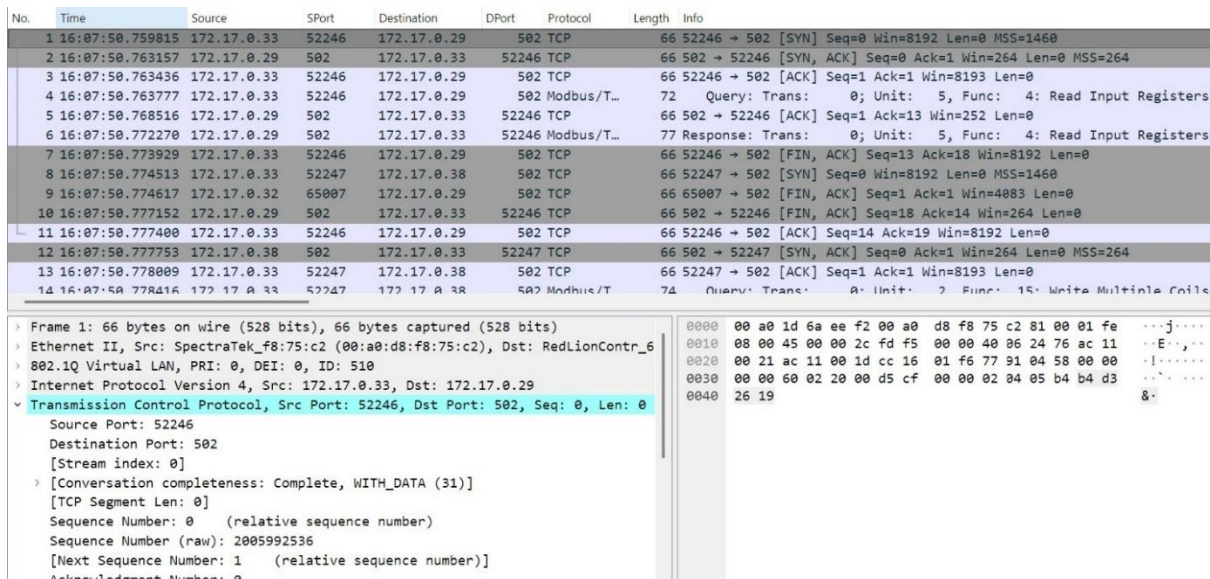


Fig. 9: Sample Wireshark PCAP file of SCADA Datasets screenshot

Fig. 9 shows a standard Wireshark packet-sniffing display pane.

#### Packet List Pane (Top Pane – Main Pane)

This is the primary pane, Table 2, and shows a summary of every captured packet—one row per packet.

It provides a chronological view of network activity

Enables filtering, sorting, and searching

Used for:

- Traffic flow inspection
- Fault diagnosis
- Cybersecurity incident analysis

#### Packet Details Pane (Middle Pane)

This pane shows the decoded structure of the selected packet in a hierarchical (tree) format.

#### Typical Layers Displayed

- Frame – Capture metadata (frame length, timestamp)
- Data Link Layer – Ethernet II / VLAN
- Network Layer – IPv4 / IPv6
- Transport Layer – TCP / UDP
- Application Layer – HTTP, DNS, Modbus, DNP3, IEC-61850, etc.

Each layer can be expanded or collapsed to inspect:

- Header fields
- Flags

- Sequence numbers
- Checksums
- Protocol-specific fields

#### Packet Bytes Pane (Bottom Pane)

This pane displays the raw packet data in both:

- Hexadecimal format
- ASCII representation

#### Key Features

- Left: byte offset
- Middle: hexadecimal values
- Right: ASCII-decoded characters

Selecting any field in the Packet Details Pane highlights the corresponding bytes in this pane.

This work, which cites previous work where it is demonstrated successfully that using multiple fields of Wireshark SCADA data that are encoded in the BB84 quantum circuits, shows that encryption and decryption have been successful [55], is extended and further broadened in scope, based on four QKD protocols for comparing QBER and thus identifying the basis for selecting the best of the four in a real telemetry application. Fig. 10 depicts the workflow diagram for the SCADA dataset QKD implementation using quantum circuits for the BB84 protocol, which has been further extended to the other 3 QKD protocols for comparison using the PNNL dataset [56],[57], Day 3: a selected data set. Using Google Colab [58], Qiskit SDK [59] Simulator, the data encoded using the angle encoding technique [60] in corresponding QKD protocol quantum circuits for simulation in Qiskit. The dataset, as mentioned above, contains over 2.5 million records, and the six fields of the PCAP packet data are represented by the corresponding six variables, derived from the PCAP file converted to CSV format. Real quantum hardware is, though, readily available; however, error correction and hardware compatibility with circuit design sensitivity is a growing research areas for large-scale implementation purposes [61].

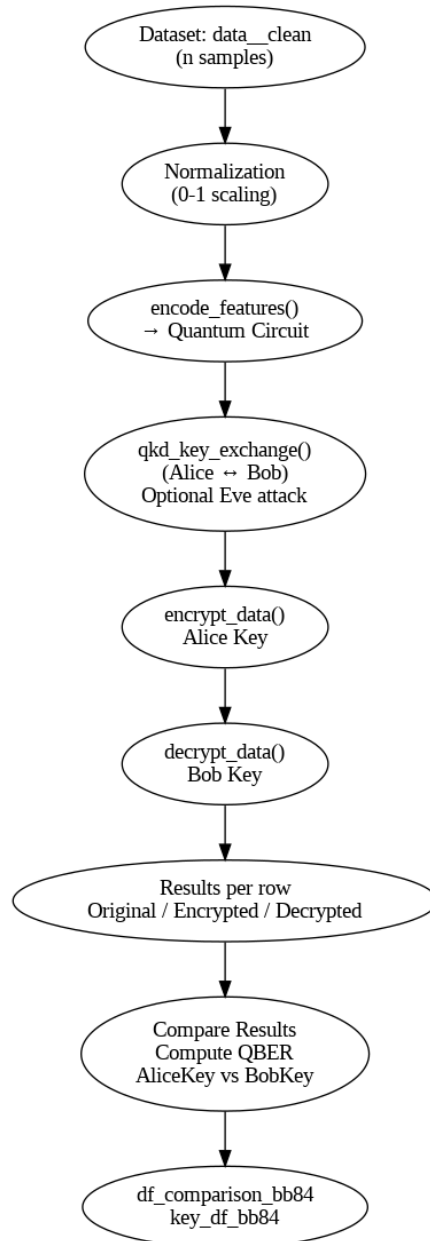


Fig. 10: Flowchart of the Implementation

Fig. 10 depicts the entire simulation process of a secure communication system based on QKD and incorporating quantum-feature encoding. After cleaning and normalising the dataset (0–1 scaling), `encode_features()` encodes classical features into a quantum circuit. Alice and Bob exchange keys using a QKD protocol (`qkd_key_exchange()`), which can optionally mimic an Eve assault. Bob uses his key to decode the data after Alice uses hers to encrypt it, and the outcomes are compared row by row. Lastly, comparison dataframes for security analysis are generated by evaluating key consistency (AliceKey vs. BobKey) and QBER (Quantum Bit Error Rate). The approach has been iterated for all the four QKD protocols.

The following equations were used in the background to derive the quantum circuits for each protocol, customized to use the six fields of the SCADA data.

Normalization:

$$f_i^{normalized} = \frac{f_i - \min(f)}{\max(f) - \min(f)} \quad (1)$$

Rotation Angle:

$$\theta_i = \pi * f_i^{normalized} \quad (2)$$

Encryption and decryption:

$$f_i' = \begin{cases} f_i & \text{if } k_i = 0 \\ 1 - f_i & \text{if } k_i = 1 \end{cases} \quad (3)$$

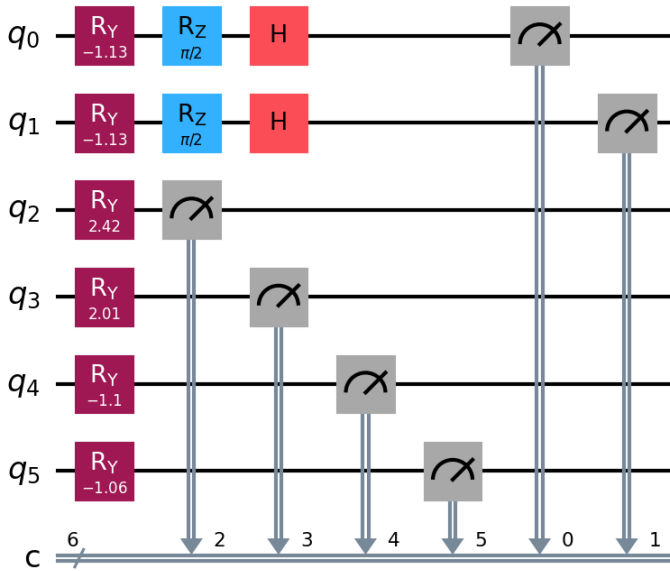


Fig. 11: A specific Quantum Circuit for the SCADA communication Data for a sample row [0]

A typical quantum circuit, as shown in Fig. 11, comprises a deep architecture of Hadamard gates, phase flips, and multi-qubit entanglement. The quantum circuit is built using Eq. 4-10.

Encoding stage:

$$\theta_i = \pi * f_i \quad (4)$$

$$R_y(\theta_i) = e^{-i\theta_i \frac{Y}{2}} \quad (5)$$

$$H = \frac{1}{\sqrt{2}} \begin{bmatrix} 1 & 1 \\ 1 & -1 \end{bmatrix} \quad (6)$$

Where the states are:

$$|0\rangle \rightarrow \frac{|0\rangle + |1\rangle}{\sqrt{2}}$$

$$|1\rangle \rightarrow \frac{|0\rangle - |1\rangle}{\sqrt{2}}$$

Controlled-X (CNOT) Gates

Entangling operations:

$$CNOT|c, t\rangle = |c\rangle \otimes X^c|t\rangle \quad (7)$$

Where X is the Pauli X-gate

Pauli Z Gate

$$Z = \begin{bmatrix} 1 & 0 \\ 0 & 1 \end{bmatrix} \quad (8)$$

The layered ansatz

$$U(\vec{\theta}) = \prod_{l=1}^L [U_{entangle}^l \cdot \otimes R(\theta_i^l)] \quad (9)$$

Where L is the number of layers, 4

The final measurement in the Z basis gives the probabilities

$$p(x) = |\langle x|U(\vec{\theta})|0^{\otimes n}\rangle|^2 \quad (10)$$

Where x is the bitstring outcome

Fig. 11, a simpler approach for this quantum feature-encoding of SCADA data using single-qubit rotation gates. Each horizontal line represents a qubit, and each qubit is equal to one SCADA variable (six qubits are equal to six variables). The Ry encodes the numerical value of that SCADA variable into the quantum state of each qubit by rotating along the Y-axis of the Bloch sphere when a  $(\theta)$  gate is applied to each qubit. In practice, the conventional SCADA readings are normalized to a certain range and then mapped to a rotation angle  $\theta$  ( $\theta$ ). A small angle retains the qubit close to the  $|0\rangle$  state, suggesting a low or nominal value, whereas a larger angle (radians) rotates the qubit closer to  $|1\rangle$ , indicating a higher or more extreme measurement. Following encoding, the probability of measuring 1 on each qubit instantly reflects the magnitude of the associated SCADA variable. This circuit creates a six-qubit quantum state from six classical SCADA variables. In short, each qubit is a quantum rotation stored as a single SCADA measurement's tiny, probabilistic carrier. To achieve the same outcomes, customized quantum circuits with SCADA six-variable data embedded have been created for the remaining three QKD systems: B92, E91, and SGS04; however, apart from data encoding, the rest of the circuits are tailored to these systems.

## Results & Discussion

Based on the above approach in the previous section, the following results surface as given below:

Table 2: Four protocols —sample 5 rows of QKD comparison

	Index	AliceKey	BobKey	KeySize	KeysMatch	QBER
<b>BB84</b>						
<b>96</b>	96	00110	01110	5	False	0.20

<b>98</b>	98	01	01	2	True	0.00
<b>5</b>	5	1001	0011	4	False	0.50
<b>40</b>	40	101	100	3	False	0.33
<b>2</b>	2	0	0	1	True	0.0
<b>B92</b>						
<b>99</b>	99	0101	0101	4	True	0.0
<b>58</b>	58	10100	10100	5	True	0.0
<b>22</b>	22	1	1	1	True	0.0
<b>31</b>	31	10	10	2	True	0.0
<b>73</b>	73	000	000	3	True	0.0
<b>E91</b>						
<b>80</b>	80	100	100	3	True	0.0
<b>35</b>	35	10110	10110	5	True	0.0
<b>61</b>	61	111	111	3	True	0.0
<b>83</b>	83	10111	10111	5	True	0.0
<b>4</b>	4	0	0	1	True	0.0
<b>SGS04</b>						
<b>60</b>	60	00	10	2	False	0.50
<b>65</b>	65	0	0	1	True	0.00
<b>29</b>	29	01	01	2	True	0.0
<b>36</b>	36	010	011	3	False	0.33
<b>5</b>	5	000000	000000	6	True	0.0

Table 2 depicts the analysis outcome of the four QKD protocols, and 5 sample rows corresponding to AliceKey, BobKey, KeySize, KeyMatch, and QBER, respectively, from the 100 rows of the dataset. It summarizes the outcome of multiple quantum key distribution (QKD) key comparison instances between Alice and Bob for the sample five rows of the dataset with the corresponding BB84, B92, E91, and SGS04 technique. For each index, the bit strings generated independently by Alice and Bob are shown along with the resulting key size, and a boolean indicator specifies whether the keys match exactly. When the keys do not match, the Quantum Bit Error Rate (QBER) quantifies the fraction of mismatched bits; higher QBER values (e.g., 0.60–0.67) indicate significant discrepancies likely due to noise or eavesdropping, whereas matching keys yield a QBER of zero, reflecting error-free key agreement.

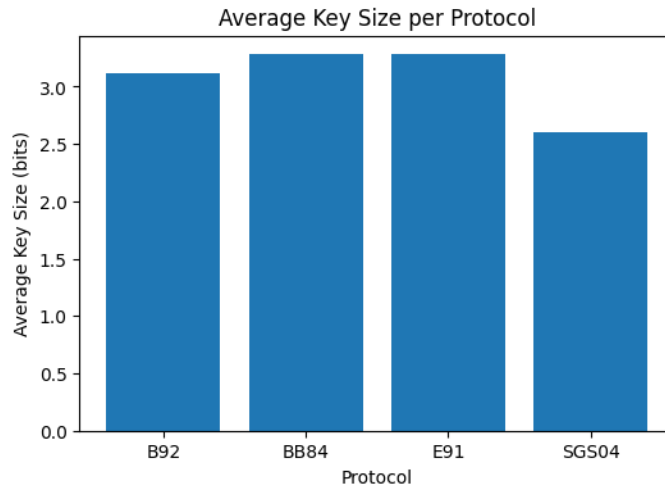


Fig. 12: Bar plot of Ave Key Size per QKD protocols

For the first 100 samples of the selected PNNL Day 3 dataset, Fig. 12 shows the average key size for each QKD protocol.

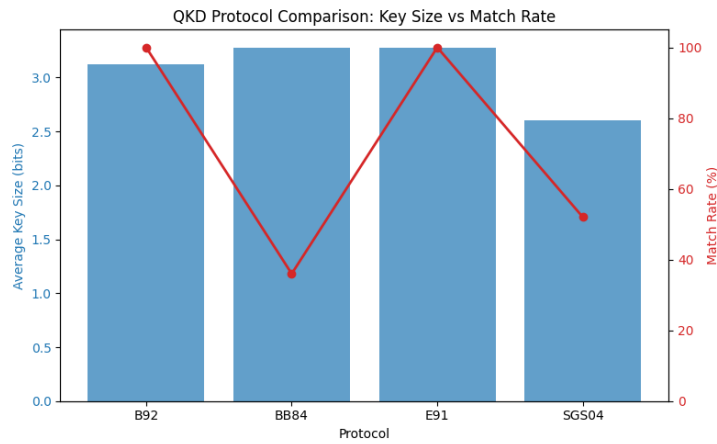


Fig. 13: Bar Plot of Key Size Vs Match Rate for All the QKD Protocols

For the first 100 samples of the Day 3 dataset, Fig. 13 shows the average key size vs. match rate percentage for the four QKD protocols.

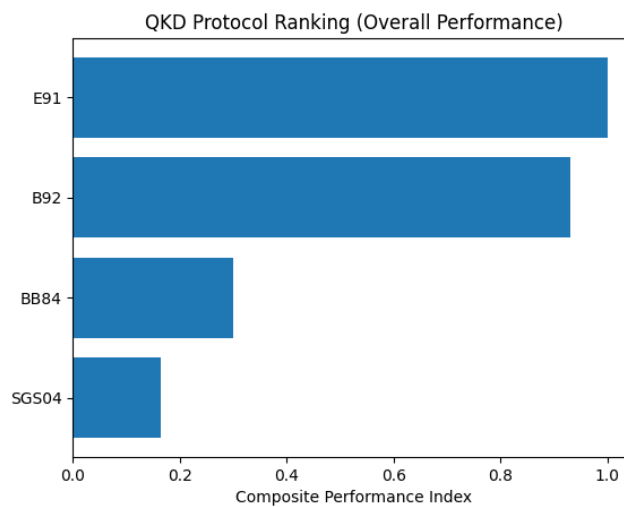


Fig. 14: Comparison Bar Chart of all the QKD protocols

Because the third protocol, BB84, achieves a large key size but performs poorly on match rate and error metrics, it is significantly skewed, suggesting that while many bits are generated, a sizable portion are unreliable, which is undesirable for practical SCADA security. In fact, this would result in frequent reconciliations or key rejections because the fourth protocol, SGS04 (red), scores poorly across all aspects, indicating poor key agreement and high inconsistency.

Not all QKD techniques scale in the same way as SCADA traffic characteristics, as the plot illustrates. techniques that balance key length with consistency and low error clearly perform better than those optimized solely for raw key generation. A composite performance index plot (Fig. 14) shows the comparison, in bars, of the four QKD protocols on the SCADA data.

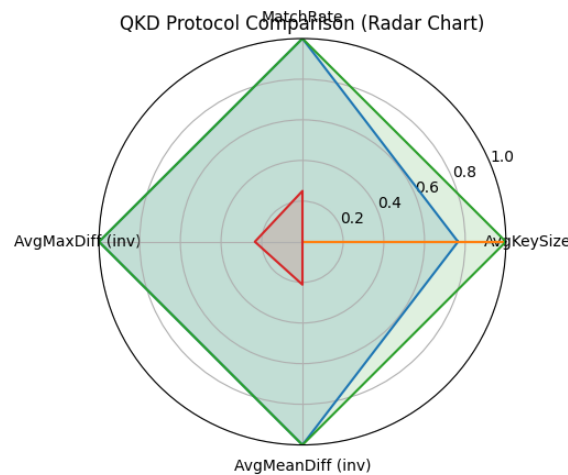


Fig. 15: Radar Chart comparing all the protocols

Fig. 15, the radar chart compares QKD techniques; the axes display the normalized performance measures i.e., KeySize, MatchRate, AvgMeanDiff, and AvgMaxDiff, and each color denotes a distinct protocol. Larger, more widely dispersed areas in protocols do better overall across all criteria. This enables rapid visual evaluation of QKD's appropriateness across different criteria, highlighting its inherent trade-offs. Clearly, the E91 protocol stands out among the others. This radar graphic illustrates trade-offs rather than absolute numbers by comparing four QKD algorithms assessed on the same SCADA dataset using four normalised performance criteria.

The best-balanced performance is achieved by a single protocol (the green trace, E91), which consistently reaches the outer boundary on all axes. It achieves the lowest key disagreement (as indicated by the inverted mean and maximum difference metrics), the largest average key size, and perfect or nearly perfect key matching. Because of this, it is the most dependable option for SCADA traffic, where steady, low-error key agreement is essential.

While maintaining a high match rate and minimal disagreement, a second protocol (blue, B92) produces a slightly smaller key size, indicating greater robustness at the expense of lower throughput. Fig. 15 further compares all QKD protocols and ranks E91 as the best overall based on the composite performance index, which corroborates Fig. 14.

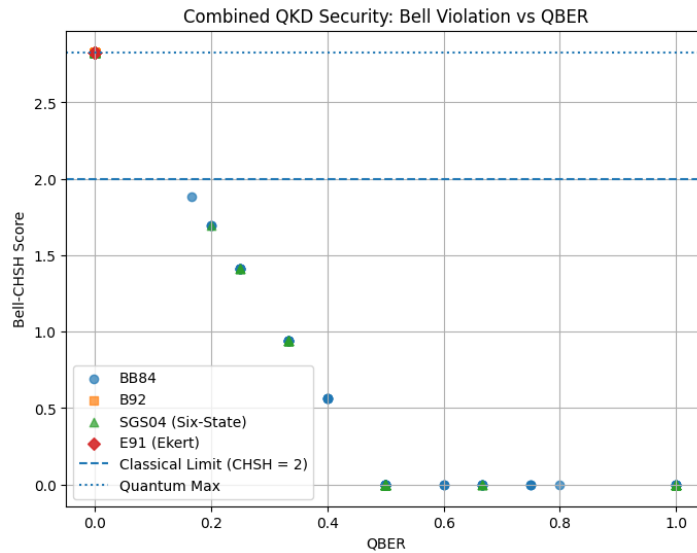


Fig. 16: Combined security for all QKD – Bell violation vs QBER

Fig. 16, using CHSH [62], a generalized Bell inequality including correlations between two particles detected under four distinct detector settings is known as the CHSH inequality, which shows that the combined Bell-violation-QBER analysis highlights E91’s unique ability to detect eavesdropping via loss of entanglement. At the same time, BB84, B92, and SGS04 rely on error-rate–based disturbance detection with differing robustness.

Table 3: IEC 62351 mapping scope

IEC 62351 Aspect	Code
Secure key establishment	BB84/B84/E91/SGS04
Attack detection	QBER
Session keys	AliceKey / BobKey
OT traffic protection	Feature encryption
Trust decision	QBER threshold

Table 4: Real fiber-based conceptual significance

QKD Code Element	Real Fiber SCADA Meaning
Qubits	Photons in fiber
Z / X basis	Polarization/phase
Eve intercept	Fiber tap / MITM
Measurement collapse	Detectable disturbance
QBER	Fiber security health

## Conclusion

The approach involves four QKD protocols to encrypt SCADA traffic features and validate security via QBER that enables the following:

- Attack-aware SCADA analytics
- Protocol-level trust scoring
- Adaptive key acceptance/rejection
- Integration with PMU/WAMS links

Across four distinct QKD protocols, key exchange over optical fiber enables intrusion-aware SCADA communication, in which QBER serves as a physical-layer trust metric before IEC-62351-compliant encryption of power system telemetry.

The results are consistent and encouraging. The approach further aligns with IEC 62351,

Table 3:

Since power system operations worldwide are fiber-optic-based, why does fiber make this practical?

- EMI immunity ensures stable quantum states
- Dedicated utility fiber for operating through a trusted channel
- Low latency implies frequent key refresh
- High availability ensures continuous QKD operation

The simulations in this work assume exactly these fiber advantages, as quantum circuits beyond simulation for actual hardware quantum computer implementation obviously entail quantum electronics due to the various intricacies underlying them.

Considering fiber-optic-based quantum communication as a secure, separate channel, it conceptually ensures the results in Table 4. As conventional cybersecurity threat entails confidentiality-integrity-availability (CIA), which in power systems applications usually comes in a reverse way, i.e., (AIC), where availability is imperative on a 24x7 basis, this work using QKD for multivariate SCADA data opens the possibility of generic use on a global scale, independent of protocols. As power system networks are designated as national critical information infrastructures (CII), this work provides a promising direction for real-world application/deployment.

For future work, we plan to extend this work to real quantum hardware and apply quantum machine learning techniques to large datasets to simulate a real-world deployment and compare the results.

## References:

- [1] M. T. Hedegaard, “Quantum encryption may secure the Danish energy grid,” pp. 5–8, 2025.

- [2] P. Evans *et al.*, “Demonstration of a Quantum Key Distribution Trusted Node on an Electric Utility Fiber Network,” *2019 IEEE Photonics Conf. IPC 2019 - Proc.*, pp. 2–3, 2019, doi: 10.1109/IPCon.2019.8908470.
- [3] M. Alshowkan, P. G. Evans, M. Starke, D. Earl, and N. A. Peters, “Authentication of smart grid communications using quantum key distribution,” *Sci. Rep.*, pp. 1–13, 2022, doi: 10.1038/s41598-022-16090-w.
- [4] D. of E. (DOE) US, “From Innovation to Practice : The CESER RMT Program ’ s Real -World Impact on Energy Sector Cybersecurity,” no. August, 2024.
- [5] D. Lakshmi, N. Nagpal, S. Chandrasekaran, and J. H. D., “A quantum-based approach for offensive security against cyber attacks in electrical infrastructure,” *Appl. Soft Comput.*, vol. 136, p. 110071, 2023, doi: 10.1016/j.asoc.2023.110071.
- [6] L. H. Nguyen *et al.*, “Towards Secured Smart Grid 2.0: Exploring Security Threats, Protection Models, and Challenges,” *IEEE Commun. Surv. Tutorials*, pp. 1–39, 2024, doi: 10.1109/COMST.2024.3493630.
- [7] K. Karabo, C. Sekga, C. Kissack, M. Mafu, and F. Petruccione, “A novel quantum key distribution resistant against large-pulse attacks,” *IET Quantum Commun.*, vol. 5, no. 3, pp. 282–290, 2024, doi: 10.1049/qtc2.12089.
- [8] A. Green, J. Lawrence, G. Siopsis, N. A. Peters, and A. Passian, “Quantum Key Distribution for Critical Infrastructures: Towards Cyber-Physical Security for Hydropower and Dams,” *Sensors*, vol. 23, no. 24, 2023, doi: 10.3390/s23249818.
- [9] N. Aquina *et al.*, “A critical analysis of deployed use cases for quantum key distribution and comparison with post-quantum cryptography,” *EPJ Quantum Technol.*, vol. 12, no. 1, 2025, doi: 10.1140/epjqt/s40507-025-00350-5.
- [10] A. Daneels and W. Salter, “What Is Scada ?,” *Int. Conf. Accel. Large Exp. Phys. Control Syst. Trieste, Italy*, pp. 339–343, 1999, [Online]. Available: <http://scholar.google.com/scholar?hl=en&btnG=Search&q=intitle:WHAT+IS+SCADA+?#0>
- [11] S. Bricker, T. Gonen, and L. Rubin, “Substation automation technologies and advantages,” *IEEE Comput. Appl. Power*, vol. 14, no. 3, pp. 31–37, 2001, doi: 10.1109/MCAP.2001.952934.
- [12] A. Shahzad, S. Musa, A. Aborujilah, and M. Irfan, “The SCADA review: system components, architecture, protocols and future security trends,” *Am. J. Appl. Sci.*, vol. 11, no. 8, p. 1418, 2014.
- [13] G. Yadav and K. Paul, “Architecture and security of SCADA systems: A review,” *Int. J. Crit. Infrastruct. Prot.*, vol. 34, 2021, doi: 10.1016/j.ijcip.2021.100433.
- [14] T. Sheldon, *McGraw-Hill’s Encyclopedia of Networking and Telecommunications*. McGraw-Hill Professional, 2001.
- [15] ITU, “Recommendation ITU-T G.652: Characteristics of a single-mode optical fibre and cable,” *Int. Telecommun. Union*, no. November 2016, pp. 1–28, 2016.
- [16] ITU-T L.151, *Recommendation ITU-T L.151 Installation of optical ground wire cable*. 2020.
- [17] H. Biswas, “Cyber Security in Power Grid Networks , At the Crossover Domain Intersection,” *2024 IEEE 5th India Counc. Int. Subsections Conf.*, pp. 1–6, 2024, doi: 10.1109/INDISCON62179.2024.10744312.
- [18] K. Scarfone and P. Mell, “Guide to Intrusion Detection and Prevention Systems (IDPS),” *Natl. Inst. Stand. Technol.*, vol. 800–94, no. February, p. 127, 2007, [Online]. Available: <http://csrc.nsl.nist.gov/publications/nistpubs/800-94/SP800-94.pdf>

- [19] D. Salmon, M. Zeller, A. Guzman, V. Mynam, and M. Donolo, "Mitigating the aurora vulnerability with existing technology," *36th Annu. West. Prot. Relay Conf.*, no. October 2009, pp. 1–7, 2009.
- [20] H. Biswas, "Malware Trend in Smart Grid Cyber Security," *2024 IEEE Reg. 10 Symp.*, pp. 1–5, 2024, doi: 10.1109/TENSYMP61132.2024.10752141.
- [21] S. Nazir, S. Patel, and D. Patel, "Assessing and augmenting SCADA cyber security: A survey of techniques," *Comput. Secur.*, vol. 70, pp. 436–454, 2017, doi: <https://doi.org/10.1016/j.cose.2017.06.010>.
- [22] L. Rosa, M. Freitas, S. Mazo, E. Monteiro, T. Cruz, and P. Simoes, "A Comprehensive Security Analysis of a SCADA Protocol: From OSINT to Mitigation," *IEEE Access*, vol. 7, pp. 42156–42168, 2019, doi: 10.1109/ACCESS.2019.2906926.
- [23] W. Luo *et al.*, "Recent progress in quantum photonic chips for quantum communication and internet," *Light Sci. Appl. 2023 121*, vol. 12, no. 1, pp. 1–22, 2023, doi: 10.1038/s41377-023-01173-8.
- [24] M. Hayashi and R. Nakayama, "Security analysis of the decoy method with the Bennett-Brassard 1984 protocol for finite key lengths," *New J. Phys.*, vol. 16, no. 21, pp. 24550–24565, 2014, doi: 10.1088/1367-2630/16/6/063009.
- [25] M. Lucamarini *et al.*, "Efficient decoy-state quantum key distribution with quantified security," *Opt. Express*, vol. 21, no. 21, p. 24550, 2013, doi: 10.1364/oe.21.024550.
- [26] Y. Zhang *et al.*, "Long-Distance Continuous-Variable Quantum Key Distribution over 202.81 km of Fiber," *Phys. Rev. Lett.*, vol. 125, no. 1, 2020, doi: 10.1103/PHYSREVLETT.125.010502.
- [27] Y. Zhang, Y. Bian, Z. Li, S. Yu, and H. Guo, "Continuous-variable quantum key distribution system: Past, present, and future," *Appl. Phys. Rev.*, vol. 11, no. 1, pp. 1–55, 2024, doi: 10.1063/5.0179566.
- [28] L. Zhou *et al.*, "Experimental Quantum Communication Overcomes the Rate-Loss Limit without Global Phase Tracking," *Phys. Rev. Lett.*, vol. 130, no. 25, p. 250801, 2023, doi: 10.1103/PHYSREVLETT.130.250801/FIGURES/4/THUMBNAIL.
- [29] "Researchers demonstrate the UK's first long-distance ultra-secure communication over a quantum network."
- [30] P. Mantri, K. Goodenough, and D. Towsley, "Comparing one- and two-way quantum repeater architectures," *Commun. Phys.*, vol. 8, no. 1, pp. 1–14, 2025, doi: 10.1038/S42005-025-02222-X;SUBJMETA=259,481,483,639,766;KWRD=INFORMATION+THEORY+AND+COMPUTATION,QUANTUM+INFORMATION.
- [31] K. Azuma *et al.*, "Quantum repeaters: From quantum networks to the quantum internet," *Rev. Mod. Phys.*, vol. 95, no. 4, p. 45006, 2023, doi: 10.1103/REVMODPHYS.95.045006/FIGURES/23/THUMBNAIL.
- [32] B. Li, K. Goodenough, F. Rozpędek, and L. Jiang, "Generalized Quantum Repeater Graph States," *Phys. Rev. Lett.*, vol. 134, no. 19, p. 190801, 2025, doi: 10.1103/PHYSREVLETT.134.190801/FIGURES/2/THUMBNAIL.
- [33] J. M. Thomas *et al.*, "Quantum teleportation coexisting with classical communications in optical fiber," *Opt. Vol. 11, Issue 12, pp. 1700-1707*, vol. 11, no. 12, pp. 1700–1707, 2024, doi: 10.1364/OPTICA.540362.
- [34] J. Yang *et al.*, "High-rate intercity quantum key distribution with a semiconductor single-photon source," *Light Sci. Appl. 2024 131*, vol. 13, no. 1, pp. 1–10, 2024, doi:

10.1038/s41377-024-01488-0.

- [35] W. Heisenberg, “Über den anschaulichen Inhalt der quantentheoretischen Kinematik und Mechanik,” *Zeitschrift für Phys.*, vol. 43, no. 3, pp. 172–198, 1927, doi: 10.1007/BF01397280.
- [36] W. K. Wootters and W. H. Zurek, “A single quantum cannot be cloned,” *Nature*, vol. 299, no. 5886, pp. 802–803, 1982, doi: 10.1038/299802a0.
- [37] G. Brassard, “Quantum Communication Complexity,” *Found. Phys.*, vol. 33, no. 11, pp. 1593–1616, 2003, doi: 10.1023/A:1026009100467.
- [38] S. Ghosh, M. Zaman, R. Joshi, and S. Sampalli, “Multi-Phase Quantum Resistant Framework for Secure Communication in SCADA Systems,” *IEEE Trans. Dependable Secur. Comput.*, vol. 21, no. 6, pp. 5461–5478, 2024, doi: 10.1109/TDSC.2024.3378474.
- [39] S. Ghosh, M. Zaman, B. Plourde, and S. Sampalli, “A Quantum-Based Signcryption for Supervisory Control and Data Acquisition ( SCADA ) Networks,” pp. 1–27, 2022.
- [40] L. K. Grover, “A fast quantum mechanical algorithm for database search,” pp. 212–219, 1996, doi: 10.1145/237814.237866.
- [41] F. Bouchard, R. Fickler, R. W. Boyd, and E. Karimi, “High-dimensional quantum cloning and applications to quantum hacking,” no. February, pp. 1–6, 2017.
- [42] V. K. V. V. Bathalapalli, S. Mohanty, C. Pan, and E. Kougianos, “QPUF 3.0: Sustainable Cybersecurity of Smart Grid through Security-By-Design based on Quantum-PUF and Quantum Key Distribution,” pp. 935–940, Jun. 2025, doi: 10.1145/3716368.3735275.
- [43] M. T. Naz, W. Elmedany, and M. Ali, “Securing SCADA systems in smart grids with IoT integration: A Self-Defensive Post-Quantum Blockchain Architecture,” *Internet Things (The Netherlands)*, vol. 28, no. February, p. 101381, 2024, doi: 10.1016/j.iot.2024.101381.
- [44] D. Upadhyay, S. Ghosh, H. Ohno, M. Zaman, and S. Sampalli, “Securing industrial control systems: Developing a SCADA/IoT test bench and evaluating lightweight cipher performance on hardware simulator,” *Int. J. Crit. Infrastruct. Prot.*, vol. 47, p. 100705, 2024, doi: <https://doi.org/10.1016/j.ijcip.2024.100705>.
- [45] B. Wyrzykowska, H. Szczepaniuk, E. K. Szczepaniuk, A. Rytko, and M. Kacprzak, “Intelligent Energy Management Systems in Industry 5.0: Cybersecurity Applications in Examples,” *Energies 2024, Vol. 17, Page 5871*, vol. 17, no. 23, p. 5871, 2024, doi: 10.3390/EN17235871.
- [46] D. Pliatsios, P. Sarigiannidis, T. Lagkas, and A. G. Sarigiannidis, “A Survey on SCADA Systems: Secure Protocols, Incidents, Threats and Tactics,” *IEEE Commun. Surv. Tutorials*, vol. 22, no. 3, pp. 1942–1976, 2020, doi: 10.1109/COMST.2020.2987688.
- [47] S. Aggarwal and G. Kaddoum, “Authentication of Smart Grid by Integrating QKD and Blockchain in SCADA Systems,” *IEEE Trans. Netw. Serv. Manag.*, vol. 21, no. 5, pp. 5768–5780, 2024, doi: 10.1109/TNSM.2024.3423762.
- [48] M. Alanazi, A. Mahmood, and M. J. M. Chowdhury, “SCADA vulnerabilities and attacks: A review of the state-of-the-art and open issues,” *Comput. Secur.*, vol. 125, 2023, doi: 10.1016/j.cose.2022.103028.
- [49] M. Mingze, “Research and Application of Firewall Log and Intrusion Detection Log Data Visualization System,” *IET Softw.*, vol. 2024, no. 1, 2024, doi: 10.1049/2024/7060298.
- [50] T. S. Ustun and S. M. S. Hussain, “IEC 62351-4 Security Implementations for IEC 61850 MMS Messages,” *IEEE Access*, vol. 8, pp. 123979–123985, 2020, doi: 10.1109/ACCESS.2020.3001926.

- [51] C. H. Bennet and G. Brassard, “Quantum cryptography: Public key distribution and coin tossing,” 1984.
- [52] C. H. Bennett, “Quantum cryptography using any two nonorthogonal states,” *Phys. Rev. Lett.*, vol. 68, no. 21, pp. 3121–3124, May 1992, doi: 10.1103/PhysRevLett.68.3121.
- [53] A. K. Ekert, “Quantum cryptography based on Bell’s theorem,” *Phys. Rev. Lett.*, vol. 67, no. 6, pp. 661–663, Aug. 1991, doi: 10.1103/PhysRevLett.67.661.
- [54] V. Scarani, A. Acín, G. Ribordy, and N. Gisin, “Quantum Cryptography Protocols Robust against Photon Number Splitting Attacks for Weak Laser Pulse Implementations,” *Phys. Rev. Lett.*, vol. 92, no. 5, p. 57901, Feb. 2004, doi: 10.1103/PhysRevLett.92.057901.
- [55] H. Biswas, “Power networks SCADA communication cybersecurity, a Qiskit implementation,” *J. Supercomput.*, vol. 81, no. 13, p. 1262, 2025, doi: 10.1007/s11227-025-07758-x.
- [56] “Electricity and Gas IDS | Datahub.” Accessed: Jan. 07, 2024. [Online]. Available: <https://data.pnnl.gov/group/nodes/dataset/13470>
- [57] T. W. Edgar, “PNNL Electricity and Natural Gas System Dataset Documentation,” no. April, 2020.
- [58] “Welcome To Colaboratory - Colab.” Accessed: Apr. 22, 2024. [Online]. Available: <https://colab.research.google.com/notebooks/welcome.ipynb>
- [59] Qiskit Team, “Release News: Qiskit SDK v2.0 is here!”
- [60] H. Biswas, “Data Encoding for VQC in Qiskit , A Comparison With Novel Hybrid Encoding,” 2025, [Online]. Available: <https://arxiv.org/abs/2503.14062>
- [61] H. Biswas, “Comparing a Few Qubit Systems for Superconducting Hardware Compatibility and Circuit Design Sensitivity in Qiskit”, doi: <https://arxiv.org/pdf/2506.14075>.
- [62] J. F. . Clauserf;, M. A. Horne, Abner Shimony;, and R. A. Holt, “PROPOSED EXPERIMENT TO TEST LOCAL HIDDEN-VARIABLE THEORIES,” vol. 23, no. 15, pp. 880–884, 1969.